UNIVERSITY OF BUCHAREST
FACULTY OF CHEMISTRY
PhD SCHOOL OF CHEMISTRY

PhD THESIS SUMMARY

NANOSTRUCTURED BIOSURFACES FOR DETECTION OF THE IMPORTANT BIOMARKERS AND PATHOGENS IN LABORATORY DIAGNOSIS

PhD Candidate,
MIHĂILESCU CARMEN-MARINELA

Scientific Adviser,
Prof. dr. BACIU ION

Reviewers: **Associate.dr. Mihailciuc Constantin (University of Bucharest)**
CSI dr. Spătaru Nicolae (Institute of Physical Chemistry "Ilie Murgulescu")
Prof.dr. Ion Alina Catrinel (Polytechnic University of Bucharest)

BUCHAREST
2015

TABLE OF CONTENTS[1]

[1]The numbering of tables, figures and references is the one from the PhD thesis

Introduction

The nanomedicine field applied on in vitro diagnostic devices (IVD) is of great interest worldwide because it presents obvious advantages: quality / price excellent, fast response, sensitivity and specificity and, of course, a very low environmental impact. These miniaturized analytical devices are already being used in medical labs outside the country (and a few in the country, particularly devices used in genomics), statistical data for the next 10-15 years indicating an explosion in this area. The field of nanotechnology involves the simultaneous use of knowledge from many fields and scientific disciplines: medicine, physics, chemistry, biology, mathematics, engineering sciences etc. The miniaturization, parallelism and integration of several functions in a single device based on techniques from the electronics industry, led to a new generation of devices small, fast, sensitive, specific and inexpensive, such as biosensors. Gradually they will replace many of the current methods obsolete and laborious with new analytical methods în clinical laboratories. Not many researchers have understood that when it refers to the manufacture of a biosensor (immunosensors) should relate to everything contained in it entirely, not only separate functionalization strategies, connections, sensors etc. Definition of biosensor according to IUPAC, says: the biosensors are analytical compact devices whose bio receptors (antibodies, enzymes, pathogens etc.) are integrated or are in direct contact with a physicochemical transducer (electrochemical, optical, thermal, piezoelectric, etc.) which converts the biological signal to a measurable analytical signal [1, 2]. This is the definition from which we started when we began studies in this thesis. When the biological recognition elements are the antibodies to specific antigens in the test sample, the sensors are called the affinity immunosensors because it can get a specific response using immune reaction based on the affinity between antigen and antibody.

Thesis objectives

The aim of the thesis was to create and to test of the biosurfaces for electrochemical immunosensors and for microarray chips with increased sensitivity and specificity, which may replace many of the current methods obsolete and laborious. These will require new analytical devices with degree of applicability in laboratory diagnosis. The main objective of this thesis is to experiment the strategies for achieve nano structured biosurfaces for development of electrochemical biosensors and microarray biochips with viable applications in laboratory diagnosis.

The proposed strategies have shown a high degree of complexity due primarily interdisciplinary methods applied specific technology development, with the deposition of antibodies and antigens, with the preparation of reagents and techniques with the use of functionalized self-assembled monolayers based the formation of (SAMs) for specific detection electro / optic of an important cardiac marker of myocardial infarction, heart fatty acid binding protein and a bacteria with dangerous to public health, the bacterium *Escherichia coli* O157: H7.

Thesis Content

Due to different strategies of approaching the subject, namely, the specific development of the bio surfaces for immunosensors with electrochemical detection and the development of bio surfaces for microarray with optical fluorescence detection, the thesis structure is different from the usual structure. Since both analytes, the pathogenic bacteria, E. coli O157: H7 and the cardiac marker protein for fatty acid-binding, heart fraction(h FABP), are different in structure and biological function, they require two different approaches to achieve bio surfaces and to create their specific experimental conditions that do to not interfere very much in changing the three-dimensional structure of such analytes. Thus **in the first chapter**, the literature data, describe the construction of such devices starting from the biological sample and ending with the moment of the detection. In addition to this general part (chapter 1) with literature data, the other chapters contain an introduction on the issues treated and the original results obtained for each proposed objective.

Chapter 2, in the section "Experimental part" presents optimization of the bio interfaces for detection of h FABP cardiac marker protein depending of its specific structure and its size. Choosing this biomarker was justified by the particular importance which it has in the diagnosis of acute myocardial infarction (AMI) where its concentration in the blood increases before other cardiac biomarkers. But for its detection it needs a very sensitive method because it has a very low molecular weight compared with other biomarkers. The techniques with the formation of the simple and homogeneous monolayers (SAMMs) and also the mixed monolayers (SAMs) can provide, in addition to being easy to achieve (a feature especially important when it want to commercialize the device) can be performed and adapted depending on the chosen biomarkers characteristics.

To determine a specific type of SAM, formed by adsorption of molecules mixed (mSAM) or a homogenous monolayer molecules, the simple (hSAM), suitable with the electrochemical direct detection of the protein h FABP, the nano structurated gold surfaces were functionalized with a mixture solution of thiols and a homogeneous solution thiols formed by a single thiol. The mixture solution of thiol is consisting from 11-mercaptoundecanoic acid (11MUA) and alcohol 3-mercaptopropanol (3MPOH) in the molar ratio 9: 1 (3MPOH: 11MUA) and the formed monolayer was named mSAM2. 11MUA functionalized surfaces were named hSAM. The time of immersion was also an important parameter in the study.

The efficiency of the formation of monolayers on gold electrodes (nano-structured gold surfaces) can be demonstrated by the ability of monolayers to block the redox reaction and can be expressed by comparing the peak separation of the anode and cathode by the ΔEp ($Ep_a - Ep_c$) obtained after each immersion time.

In Fig. 2.20 (a, b) the cyclic voltammograms, who enabling the formation of SAMs batches after each time of imersion : 1 minute, 10 minutes, 30 minutes and 16 hours, were present. After 1 minute there is a rapid decrease in current anodic and cathodic for hSAM. After 10 minutes already no longer observed any reaction of the redox couple, the monolayer becoming non-conductive. By comparison, for the monolayer $mSAM_2$, the total blocking of the current it is not achieved even no after a longer immersion. Always there will exist the transfer charge to the electrode surface which makes that this monolayer can not be used for developing the capacitive immuno sensor for detection of protein h FABP since the flaws allow the electron transfer to and from the electrode surface therefore showing an increasing of the capacity instability.

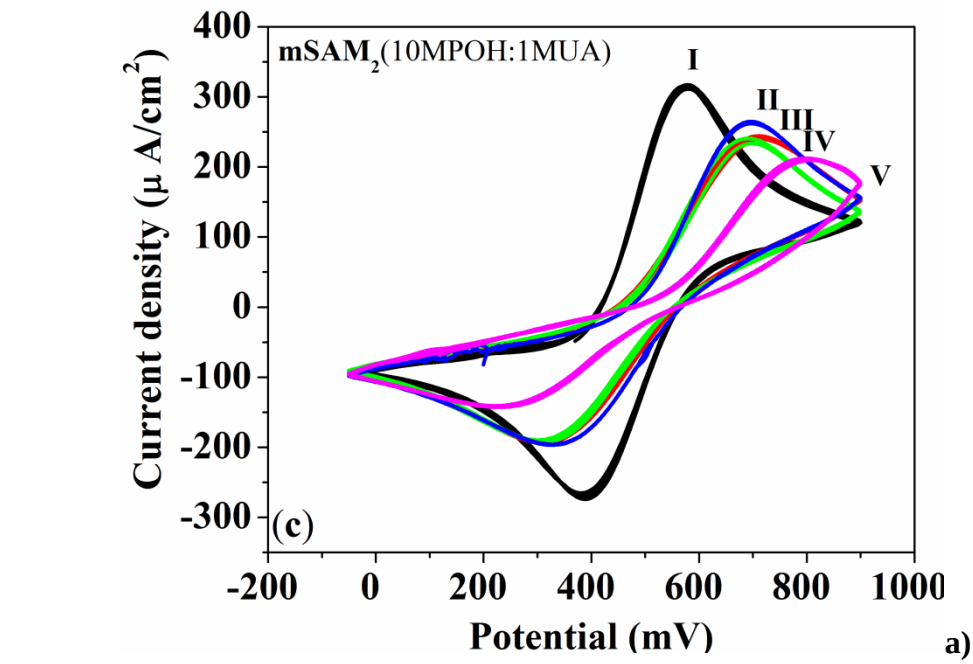

a)

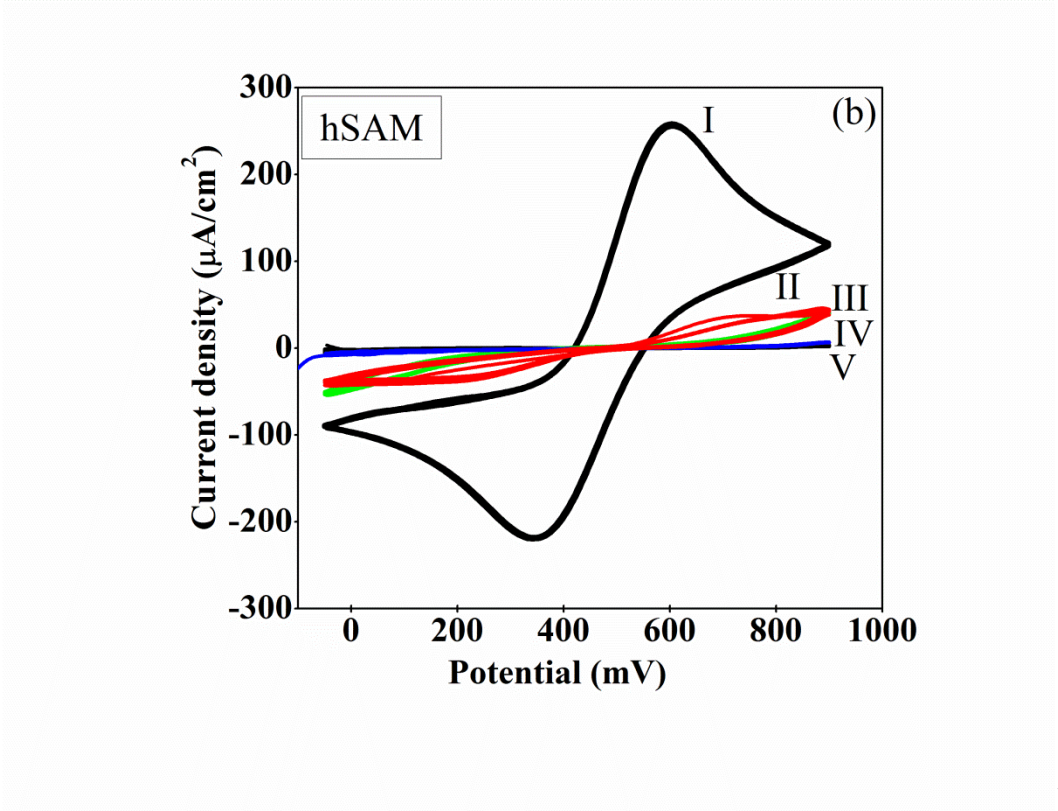

b)

Fig. 2.20 Cyclic voltammograms of the (a) $mSAM_2$, (b)hSAM after (I) bare gold (II) 1 min (III) 10 min (IV) 30 min (V) 16 h. The electrolyte is PBS solution (pH=7.4) containing $Fe(CN)_6^{3-/4-}$ as a redox couple and scan rate is 100mV/s. [145]

For each SAM batch were recorded the Nyquist impedance plots (-Z' vs Z'') (shown in Fig. 2.21) corresponding to the four times of immersion and the fitting parameters were calculated with an appropriate equivalent circuit as presented in insert from Fig. 2.21. **[145].** The

obtained parameters values are consistent with observations made after the recording the voltammograms shown in Fig.2.20.

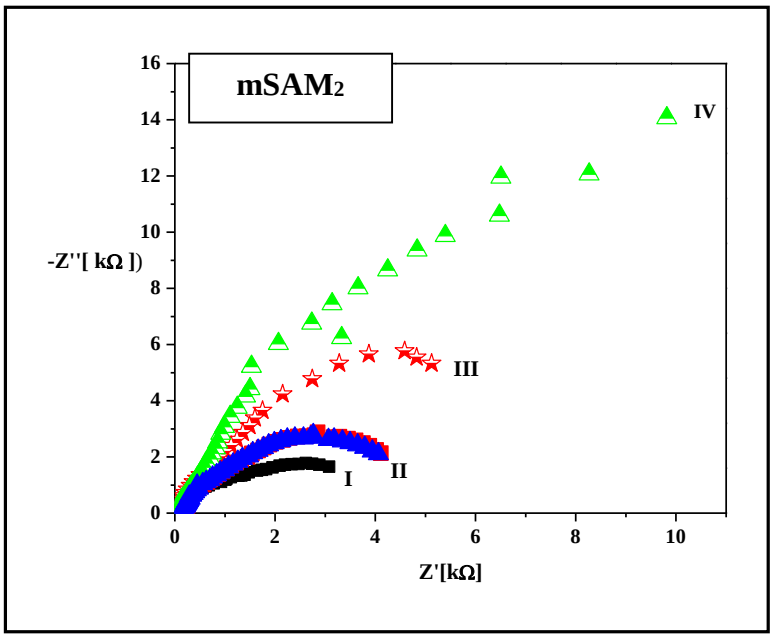

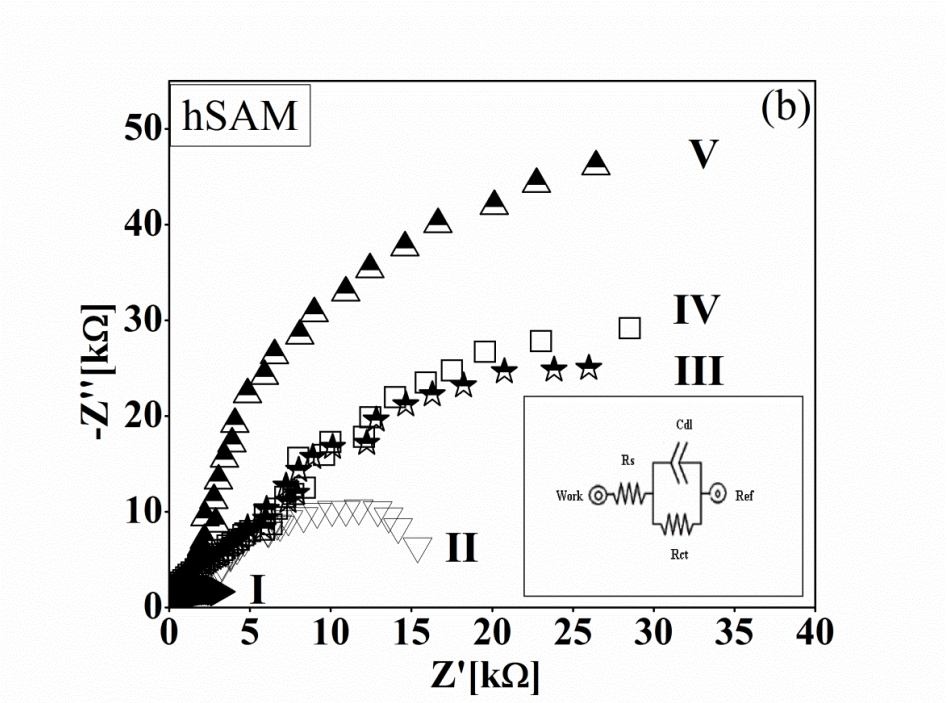

Fig. 2.21Nyquist plots (Z'' vs Z') of $mSAM_2$ and hSAM by following different immersion times: i)bare gold ii)1min iii)10 min iv)30 min v) 16h. The inset figure is the equivalent electrical circuit which includes the solution resistance (Rs), double layer capacitance (C_{dl}) electron transfer resistance (R_{ct}) [145].

The surface coverage, for all two batches of the SAMs was estimated using the equation:

$$\theta = 1 - \frac{R_{ct}}{R_{ct}^{'}}$$

where R_{ct} is the electron transfer resistance before thiol deposition and R'_{ct} is the electron transfer resistance after thiol deposition. The values for Θ, the covered area after some periods of times of homogenous hSAM and $mSAM_2$ are presented in Table 2.8.

Tabel 2.8 The percentage of covered area for hSAM and mSAM gold electrodes for different immersion period of times [145]

Immersion times	hSAMs θ (%)	$mSAM_2$ θ (%)
0	-	-
1 min	76,0	8,5
10 min	90,6	8,4
30 min	92,0	31,3
16 h	95,8	61,7

The gold electrodes were completely covered with a closely packed monolayer after 10 minutes for hSAM but the electron –transfer resistance continued to increase and it finally stabilized after 16h. The gold electrodes coverage was better after 16h immersion time in alkanetiol solutions. The final auto-assemblation for hSAM is achieved only after 16h with 95,8% the percentage of covered area. Unlike of hSAM, the Rct value for $mSAM_2$ increase slowly until at 30 minutes and achieve the maximum value only after 16 h. The self-assembling monolayer capacity is much lower than in hSAM and the surface coverage percentage reaching only 61.7% after 16 hours of immersion.

After activation with EDC/NHS, the majority of terminal carboxylic groups were converted to NHS esters, so that the repulsive interaction with anionic probe $Fe(CN)_6^{3-/4-}$ at the electrode interface will not occur, therefore the transfer of the redox ions $Fe(CN)_6^{3-/4-}$ to the electrodes surfaces was promoted.

It is observed from Figs. 2.26 and 2.27 that the monolayers became less insulating, and an increased current response was occurred **[145].**

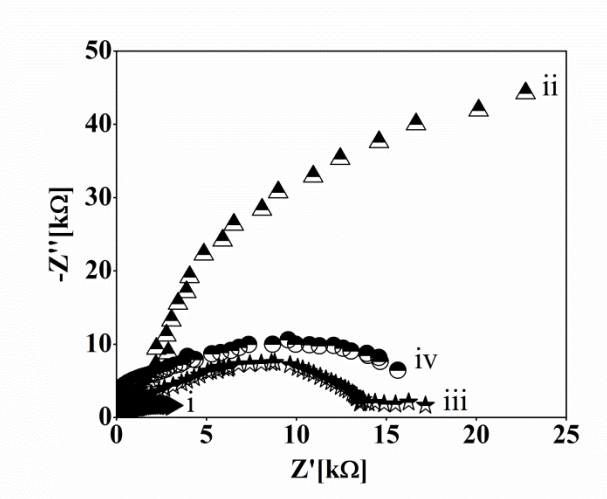

Fig. 2.26 Nyquist plots (Z' vs Z'') of gold electrode with (a) hSAM i) bare gold ii) hSAM 16h/gold electrode iii) gold /hSAM/ EDC/NHS, iv) gol electrode/ hSAM/EDC/NHS/anti-hFABP/BSA [145].

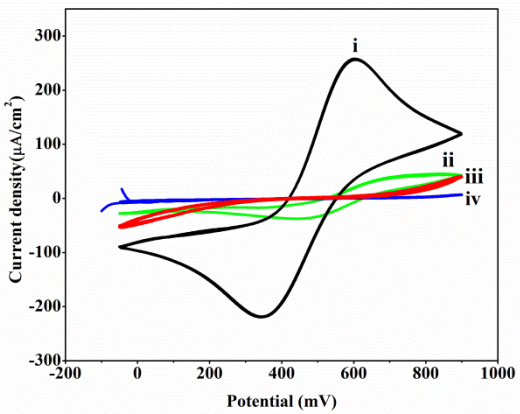

Fig. 2.27 Cyclic voltammograms of the (a) $mSAM_2$, (b)hSAM after (i) bare gold (ii)hSAM 16h/gold electrode (iii) gold /hSAM/ EDC/NHS, (IV) gol electrode/ hSAM/EDC/NHS/anti-hFABP/BSA. The electrolyte is PBS solution (pH=7.4) containing $Fe(CN)_6^{3-/4-}$ as a redox couple and scan rate is 100mV/s [145].

The EIS results show that the diameter of the semicircle of the Nyquist plots **(Z'' vs Z')** increased along with the increasing of hFABP concentration, demonstrating that the immunoreactions with anti hFABP occurred.

The corresponding Nyquist plots of impedance spectra are presented in Fig.2.32.

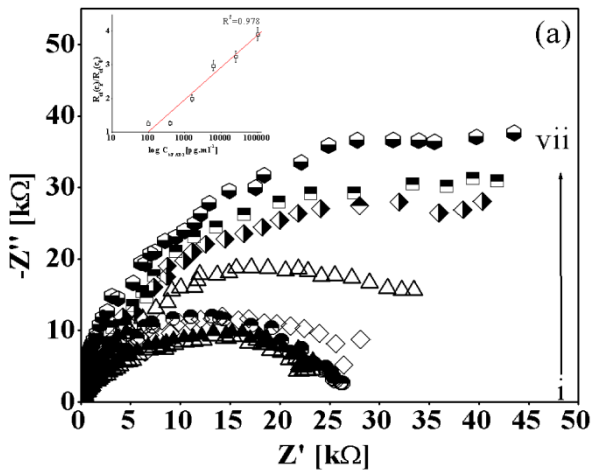

Fig. 2.32 Nyquist plots (Z''vs Z') of hSAM modified gold electrode for different hFABP/PBS concentration: i) buffer, ii) 98 $pg.ml^{-1}$, iii) 390 $pg.ml^{-1}$, iv) 1.56 $ng.ml^{-1}$, v) 6.12 $ng.ml^{-1}$, vi) 25 $ng.ml^{-1}$, vii) 100 $ng.ml^{-1}$; the insert figure is the linearity curves for normalized values obtained from EIS studies for different hFABP concentrations in PBS for hSAM [145]

To evaluate the interaction between analyte and electrode surface, normalized data were used by plotting $R_{ct}C_i$ (R_{ct} after hFABP incubation)/$R_{ct}C_0$ (R_{ct} before hFABP incubation) versus logarithm of hFABP concentration. A linear relationship was observed between the logarithm of hFABP concentration and $R_{ct}C_i/R_{ct}C_0$ values. The linear equation, correlation coefficient, detection limit and sensitivity for the hSAM are presented in Table 2. 11 **[145].**

Tabel 2.11. The curve parameters of $R_{ct}C_i/R_{ct}C_0$ versus different hFABP concentration in PBS for hSAM/EDC/NHS/anti-hFABP/BSA gold electrode

Curve parameters	Electrod hSAMs/EDC/NHS/ anti hFABP/BSA
Linear equation	$R_{ct}C_i/R_{ct}C_0$=0.891+0.954 log C_{hFABP}
Correlation coefficient	R^2= 0.978
Detection limit	524 pg.ml $^{-1}$
Sensitivity	0.954 ml.pg^{-1}

Specificity of the biosurfaces Au/hSAMs / EDC / NHS / anti-hFABP / BSA was tested by adding five protein hFABP concentrations in control human serum wich contains a variety of other analytes (enzymes, proteins, electrolytes, etc.). The study of specificity is very important because non-specific interactions between surface electrodes and other analytes in real samples of serum could lead to false positives or false negatives. Therefore, the 5 others biosurfaces, for each batch, were incubated with human serum control spiked with 5 hFABP concentrations: 98 pg / mL; 3.125 ng / mL; 12.5 ng / mL; 50 ng / mL and 100 ng / mL for 30 min at 37 ° C, and after washing with PBS, the impedance spectra were recorded. The results are shown in Fig. 2.33 **[145].**

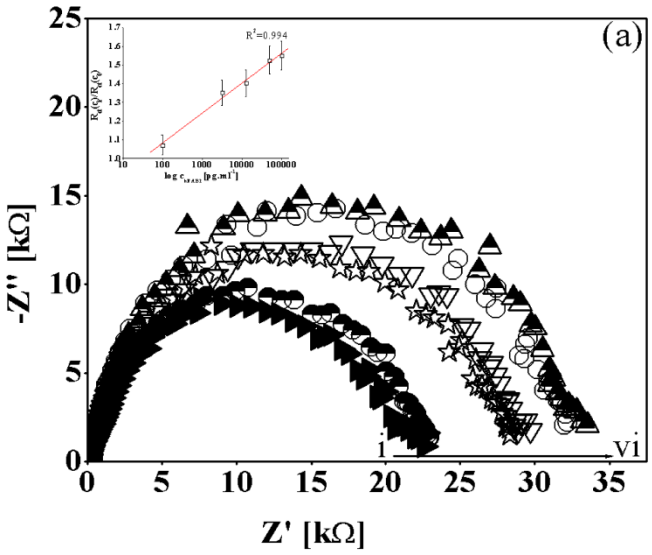

Fig. 2.33 Nyquist plots (Z''vs Z') of hSAM modified gold electrodes for different concentration of hFABP in human serum and PBS buffer (1:1): i) 0 pg.ml^{-1}, ii) 98 pg.ml^{-1}, iii) 3.125 ng.ml^{-1},iv) 12.5 ng.ml^{-1}, v) 50 ng.ml^{-1}, vi) 100 ng.ml^{-1}; the insert figure are the linearity curves for normalized values obtained from EIS studies for different hFABP concentrations in human serum for hSAM [145]

It has been shown that these biosurfaces can not be used for direct detection of the cardiac biomarker hFABP, using real samples, because there is no specificity.

In conclusion, the high ratio between 11MUA and 3MPOH is not a good choice for the detection of this biomarker because nonspecific adsorption occurs but neither maximum ratio (corresponding to $mSAM_2$ formation) between the two compounds is not a good option. Therefore, it was continued the optimization but the nanostructured biosurfaces were gold interdigitate type in order to have a better reaction time and a higher possibility of applicability în diagnostic laboratories. It was used the biosurfaces with the rate between the molecules of 7: 3 (3MPOH: 11MUA). These were named $mSAM_1$.

The successive steps of biointerface assembling, in term of changes in surface morphology, were also verified with AFM technique. For each steps of assembling were recorded FTIR - ATR spectrum and results will be presented and discussed step by step for each type of the biosurface. Determination of affinity constants of the immune response was determined by the current technic, ELISA.

Therefore to demonstrate the functionality of the nano structurated bio surfaces for detecting the hFABP these surfaces were integrated to a microfluidic platform whose block diagram is shown in Fig. 2.36.

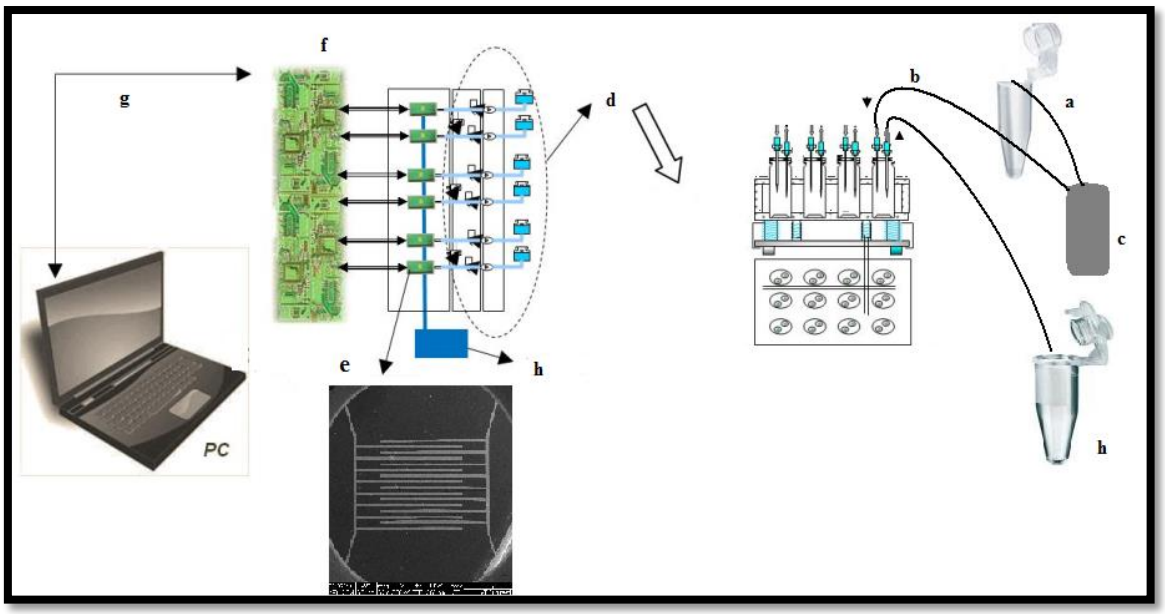

Fig. 2.35 The block diagram of the platform [147]

The block diagram of the platform: (a) container with the biological sample or washing solution; (b) transport capillary samples/washing solutions; (c) peristaltic micropumps;(d) microvalve system, canals and reservoirs; (e) immunosensor with active area represented by gold interdigitated electrodes; (f) unit for electronic measurement signal amplification Agilent; (g) PC for data recording; (h) exhaust-system for biological sample/washing liquid.

It were monitored the capacitive behavior (conductive) of the three types of functionalized surfaces with SAMs: $mSAM_1$, $mSAM_2$ and hSAM by recording the EIS spectras. It is well known that SAM is viewed as a pure capacitor and it is deemed defect free when the phase angle (φ) is ≥88º (for practical purposes), and to be a leaky capacitor when the φ value is <

87º over the 1 Hz−50 Hz range [101,146, 152]. The Bode phase Plot (φ vs frecuency) is used for monitoring the phase angle and the capacitance after various incubation times of gold surfaces with thiols solutions for further formation of $mSAM_1$, $mSAM_2$ and hSAM.

As shown in **Fig. 2.38**, the phase angle (the Bode phase plots) for all SAMs formed after adsorption during 24 h increases with time and $mSAM_1$ and hSAM become capacitors **[147].**

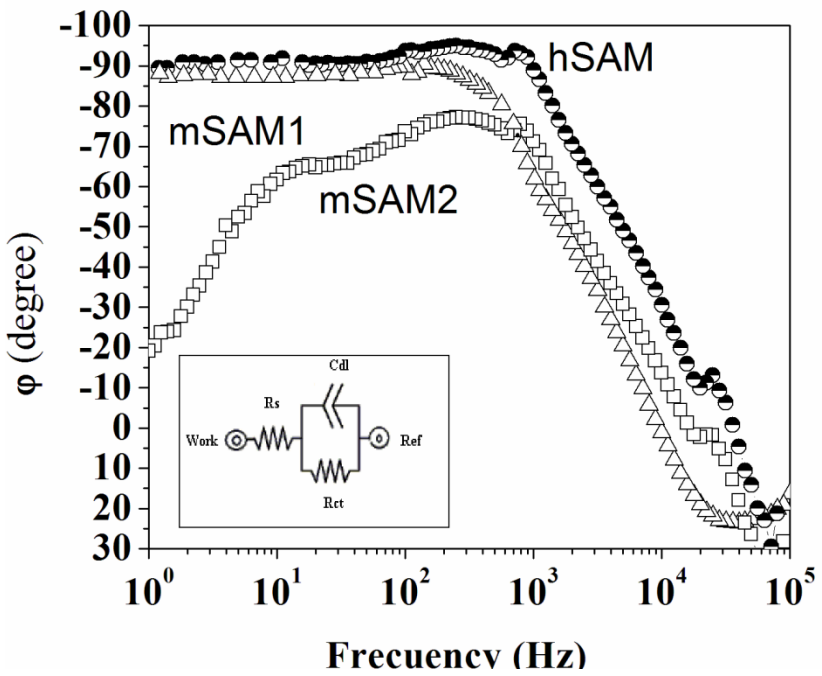

Fig. 2.38 Bode phase plots (φ vs frecuency) for $mSAM_1$, $mSAM_2$ and hSAM after 24 h immersion time in the PBS solution (pH=7.4). The inset figure is the equivalent electrical circuit with solution resistance (Rs), double layer capacitance (C_{dl}) electron transfer resistance (R_{CT}) [147].

For all bare gold electrodes modified with monolayers, a decrease in the current is produced compared to that obtained at the non-modified electrodes. This is due to the blocking proprieties of the monolayers. The decrease of the anodic and cathodic currents in the first minutes is more rapid for hSAM compared to $mSAM_1$ and $mSAM_2$. The $mSAM_2$ presents pinholes on the monolayer through which the redox probe can penetrate onto the surface, which explains why the ΔEp value is smaller than that for hSAM and $mSAM_1$, even after a long time of incubation (>20 h). These pinholes are caused by the low percent of MUA compared to MPOH that promotes the transfer of the negative redox ions $Fe(CN)_6^{3-/4-}$ to the electrode surface, thus decreasing the blocking properties of the $mSAM_2$ monolayer. Because the $mSAM_1$ monolayer shows the highest difference in the responses of bare gold vs. modified electrode, it was chosen for further development of the immunosensor.

According to the voltammetric behavior, the blocking reaction occurred more rapidly for hSAMs compared to mSAMs. The efficiency of the formation of SAMs for different immobilization times is more precisely described by the EIS results **[145]**.

For a capacitive immunosensors, an electrode is coated with an antibody, which represents the biorecognition element and has a stable capacitance. When the hFABP binds to its specific antibody on the electrode, it causes a capacitance change. The use of the second type of capacitive immunosensors, the interdigitated electrodes (IDEs), can provide a larger sensor surface for immunoreaction. The capacitance between the IDEs can be described by the Helmholtz model by equation (2.1):

$$C = \frac{A \times \varepsilon \times \varepsilon_0}{d} \quad (2.1)$$

where ε is the dielectric constant of the medium between the plates, ε_0 is the permittivity of free space, A is the area of the electrodes and d is the distance between the two electrodes.

The principle of the method of immunodetection for capacitive immunosensor is as follows: hFABP protein immobilization onto nanostructured bio surfaces $mSAM_1$ / anti-hFABP / BSA and respectively hSAM/ anti-hFABP / BSA will cause a thickness increase, which determines the changing in total capacity for each biosurface according to the equation (2.3):

$$1/Ce = 1/C_{SAM} + 1/C_{psl} + 1/C_{dl} \quad (2.3)$$

where the total capacitance is represented by the equivalent capacitance (C_e) and is built up from several components. In this case, the first is the capacitance of the monolayer, C_{SAM}. The second is the capacitance of the protein layer and any part from the Stern layer, C_{pl}. The third is the capacitance of the diffuse layer, C_{dl}.

Because these monolayers presents good insulating properties (demonstrated for $mSAM_1$ and hSAM in Bode phase diagram, Fig.2.39), this along with the capacity of diffuse layer (which is quite thin with a low solution resistance) have much higher capacities than the capacity of bio-recognition layer after immobilization of antibodies and BSA protein. If we use equation (2.3) as capacities are subunitary, we can say that the total amount of capacity is dominated by changes in capacity arising after reacting with the immobilized antibodies and hFABP protein.

The potentiostatic step method has been chosen for the capacity measurements since at a low voltage application (up to 100 mV) and at a low frequency (1 kHz) the experiments can be described as a simple RC circuit in Fig.2.41 **[147].** $mSAM_1$ resistance is much higher than the resistance due to the solution (99.97 Ω / cm^2 compared to 87.60 KΩ / cm^2). Therefore the circuit used in the EIS, with nonfaradaice conditions, is transformed into an open circuit RC series in Fig.2.41 (b) and the total capacitance changes arising at the electrode biosurfaces, after the addition of different concentrations of protein, it can be attributed to the reaction between the protein and the bio functionalized electrodes.

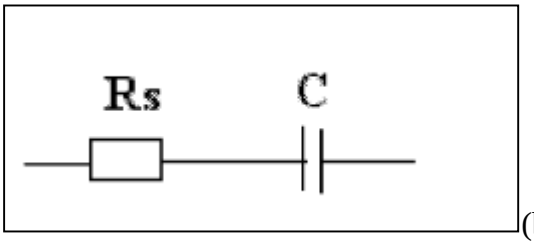

(b)

Fig. 2.41 Circuit echivalent RC ($R_{solutie}$ şi C=capacitatea totală a straturilor de pe electrozi).

After immunoreaction, the capacitance decreases with the incubation time and becomes constant after 30 min, indicating that saturation has begun. For each added concentration the capacitance change was monitored for 30 min. As it is shown in **Fig.2.41,** the fabricated immunosensor is sufficiently sensitive to exhibit a change in signal for $mSAM_1$ but also for hSAM. The thickness of the layers is a very important characteristic of a capacitive sensor. For our mixed monolayer $mSAM_1$ with short and long chain, a larger change in relative capacitance comparative with

hSAM was obtained. Under the optimization of experimental condition, for the GID electrode hSAM/h-FABP antibody and $mSAM_1$/h-FABP antibody, both blocked with BSA, it was found that the capacitance changes (ΔC) were proportional with the logarithm of h-FABP concentration in the range of 98 $pg.ml^{-1}$ to 100 $ng.mL^{-1}$in PBS buffer, as can be seen in **Figs. 4a** and **4b**. The regression equation, correlation coefficient and sensitivity for both gold electrodes surfaces are presented in Table 2.13. The limit of detection for $mSAM_1$ and hSAM was found to be approximately 3x the standard deviation of the baseline samples (with PBS) and, combined with the good linear response, yielded the values 0.836 $ng.ml^{-1}$ for $mSAM_1$ and 0.968 $ng.ml^{-1}$ for hSAM.

Tabel 2.13. The curve parameters of DC **versus different hFABP concentration in PBS for hSAM/EDC/NHS/anti-hFABP/BSA gold GID electrode [147]**

Curve parameters	hSAM/EDC/NHS/ anti hFABP/BSA GID electrode	$mSAM_1$/EDC/NHS/anti hFABP/BSA GID electrode
Linear equation	DC (nF) = -17.98–7.40 log C_{hFABP}	DC (nF) = -39.27–6.71 log C_{hFABP}
Correlation coefficient	R^2 = 0.975	R^2 = 0.981
Detection limit	968 $pg.ml^{-1}$	836 $pg.ml^{-1}$

Selectivity of the immunosensor

The selectivity of the immunosensor refers to the effect of possible interferences with the determination of the h-FABP in samples. The steric hindrance that can occur after the interaction between the h-FABP antigens with antibodies can lead to its removal from hSAM. It is evident that the interaction between anti-h-FABP and h-FABP was much strong in the case of the mSAM/anti-h-FABP as compared with hSAM/anti-h-FABP when the serum samples were used (Fig. 2.42 a and b). The steric hindrance was higher for homogenous SAMs and therefore it decreased the capacity of the anti-h-FABP antibody to bind the h-FABP antigen in human serum. The relative standard deviations (R.S.D) of the intra- and inter-assay for the immunosensors chip fabricated with $mSAM_1$ in order to detect h-FABP antigen in the linear detection range were 8 % (n=5) for intra-assay and 12.1 (n=3) for inter-assay **[147].**

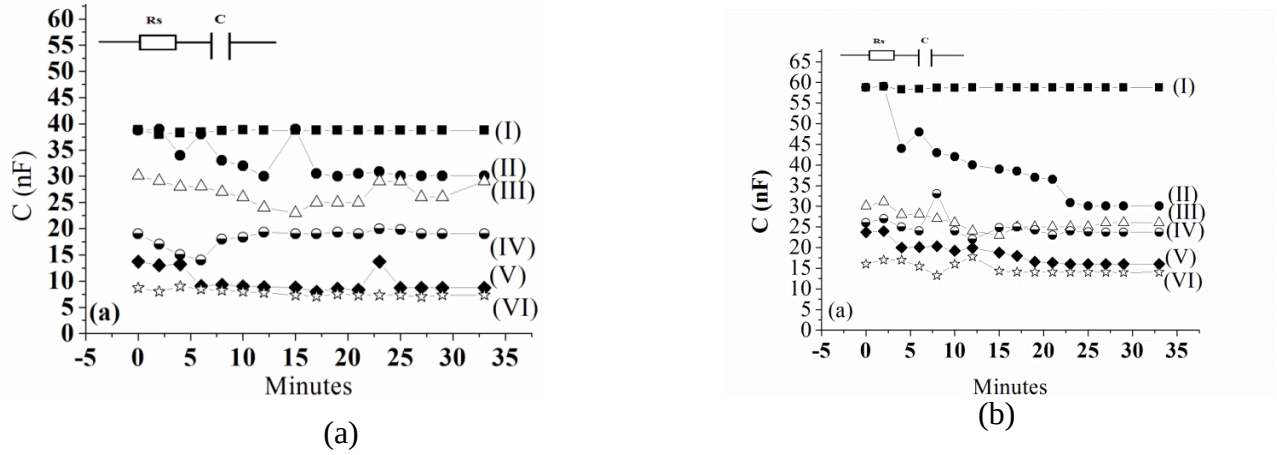

Fig. 2.42 Capacitance response of the (a) hSAM/Anti-FABP and (b) $mSAM_1$/Anti-FABP with 100 µL suctioned of (I) PBS buffer (II) 98 $ng.mL^{-1}$(III) 1.56 $ng.mL^{-1}$(IV) 3.125 $ng.mL^{-1}$(V)50 $ng.mL^{-1}$(VI) 100 $ng.mL^{-1}$. The inset figure is the RC model electrical circuit with solution resistance at the electrode surface and C is the total capacitance of the electrode layers [147];

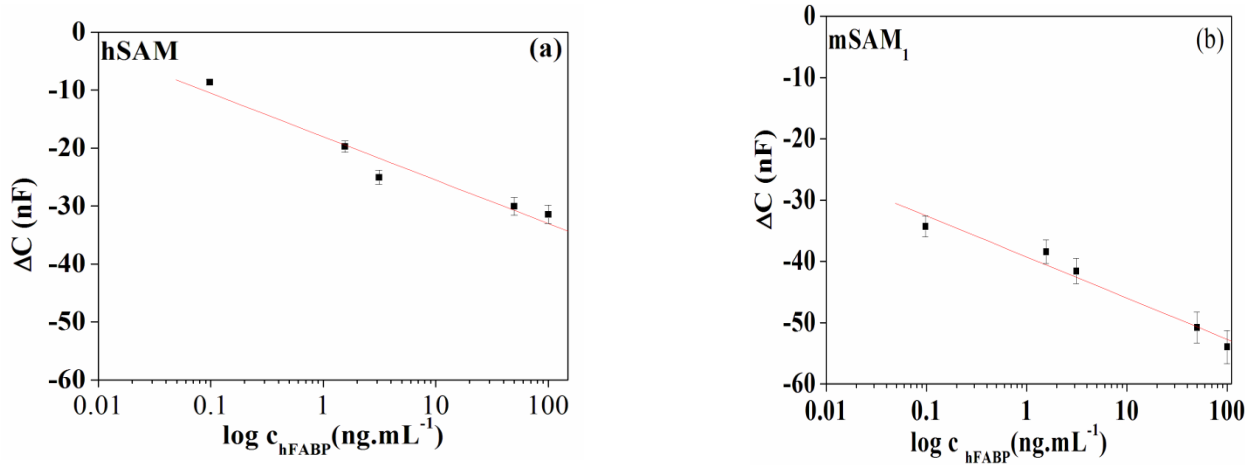

Fig.2.43 (a) The linearity curves for modified capacitances (ΔC) for different hFABP concentrations in PBS for hSAM (a) and $mSAM_1$ (b); each capacitance experiment was run in triplicate and represented with error bars.

In Chapter 3 (in the "Experimental Part"), in contrast with hFABP that has been used in the previous chapter, it was used the bacterium *E. coli* O157: H7, which is a large analyte (1-3 µm) and it must recognize his specific antibodies, covalently immobilized on a solid surface formed of with a mixed layer of organic molecules. Since the substrate was gold, we chose an organic molecule with long-chain alkanethiol (11 carbon atoms) that reacts with covalently immobilized antibacterial antibodies and another short-chain alkanethiol (3 carbon atoms) molecule, which have only the spatialization role, further for prevent the effects of steric hindrance that may arise. The ratio between the molecules has been optimized and the surfaces with the best results were used to develop the immunosensor. All stages, of functionalization with monolayers and further bio funcționalization, have been characterized by modern characterization techniques: AFM, SEM, FTIR-ATR, ellipsometry, electrochemical (CV and EIS). For each stage of the bio surface formation, Au/mSAM2/anti-E.coli /BSA, were recorded the cyclic voltammograms and were compared with voltammograms after Au/hSAM/anti-E.coli /BSA bio surface formation.

As expected, when the $mSAM_2$ layers formation occurs does not locks the total currents even after 24 hours of immersion in thiols.

After activating with EDC and NHS, an increase peak currents was observed due to the formation of sulfonic esters on the surface who stop the repulsive interactions of redox negative ions with negative ions carboxyl , these being able to more easily reach to the gold surface. There is a decrease of the conductive properties for both monolayers however an increase of the current for the hSAM were recorded higher than $mSAM_2$ because the presence of hydroxyl groups contribute with addition ionizable groupe and therefore lead to increased repulsion between ions (this was found also when was compared hSAM vs $mSAM_1$).

The covalent binding of the antibody to the surface reduces the penetration of the redox ions by the two types of surfaces, thereby reducing the current intensity.

An important information is: when blocking the surfaces with BSA the anodic peak current response is about the same value (Ia = 4 mA) for both surfaces. Therefore, although in the early stages of formation bio surfaces, their behavior is different from the electrochemical point of view, however, after blocking reactive sites on the antibody, the layers have about the same insulating properties (Fig.3.26).

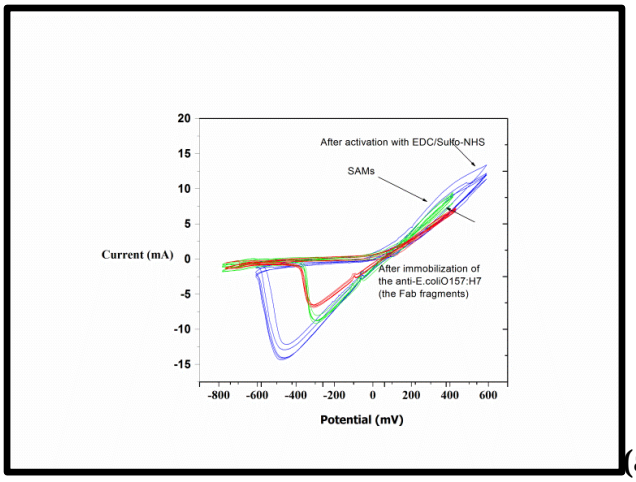

(a)[197]

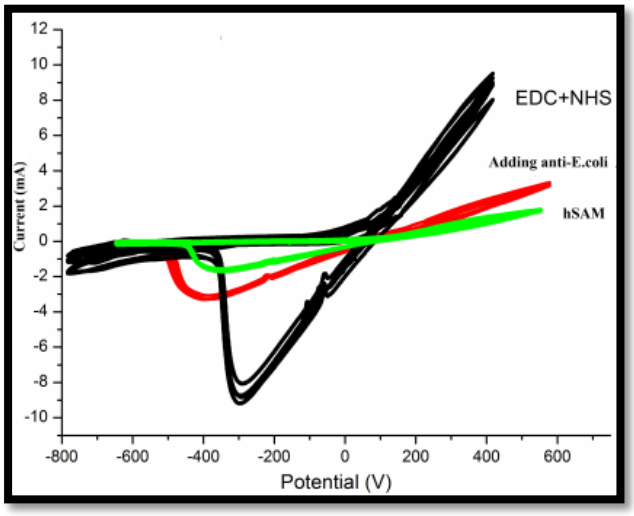

(b)

Fig. 3.26 Cyclic voltammograms of the (a) $mSAM_2$, (b)hSAM after each stage of biosurface formation; the electrolyte is PBS solution (pH=7.4) containing $Fe(CN)_6^{3-/4-}$as a redox couple and scan rate is 25 mV/s.

The surfaces morphology of SAMs formed could not be determined with SEM or AFM. In Figures 3.34 and b, it can be seen the morphology of the bacteria adsorbed on the surface with specific antibodies that have been immobilized by physical adsorption. It is obviously extremely low number of bacteria was immobilized on biosurface. Unlike the glass surface; the gold surface has a high hydrophobicity and very low degree of adsorption of the bacterial antibodies. It is clear that the gold surface requires a chemical treatment to increase adsorption of the antibodies onto surface since seen as a future bio surface for developing new immunosensor this cannot be effective.

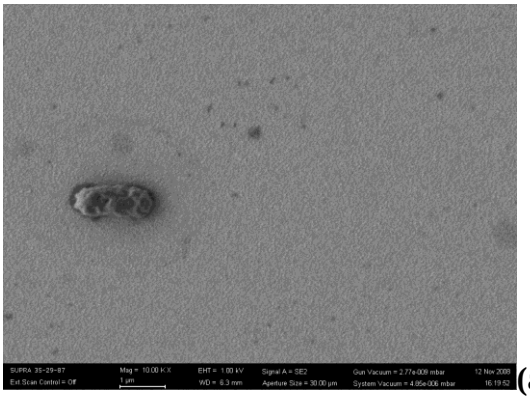

(a)

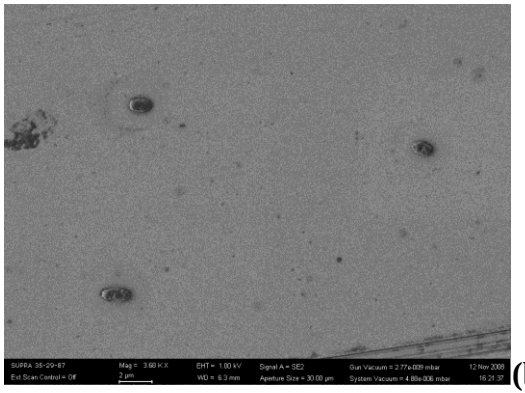

(b)

Fig. 3.34 (a,b) SEM images of bacteria immobilized by physical adsorption on gold surfaces (1 mm, and 2 µm)

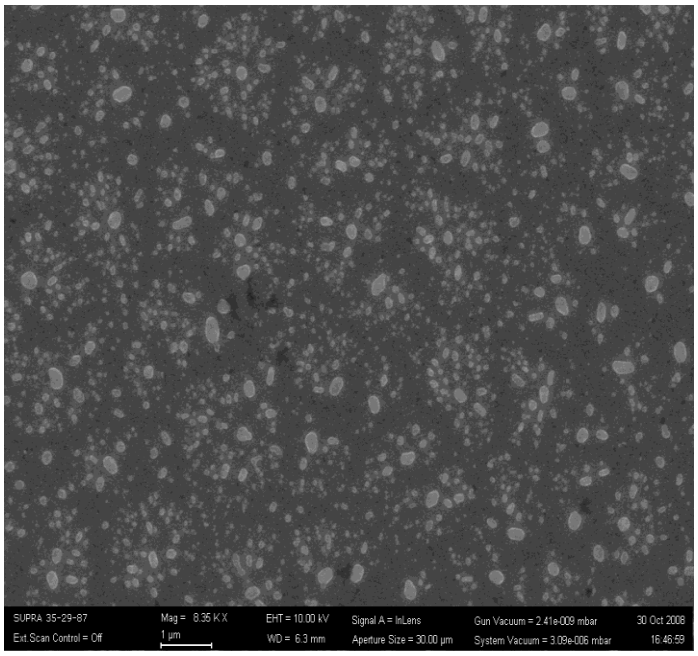

(c) [198]

Fig. 3.34 (c) SEM images of the biosurface constructed with Au / mSAM2 / antibacterial antibodies / BSA (1 mm, and 2 µm).

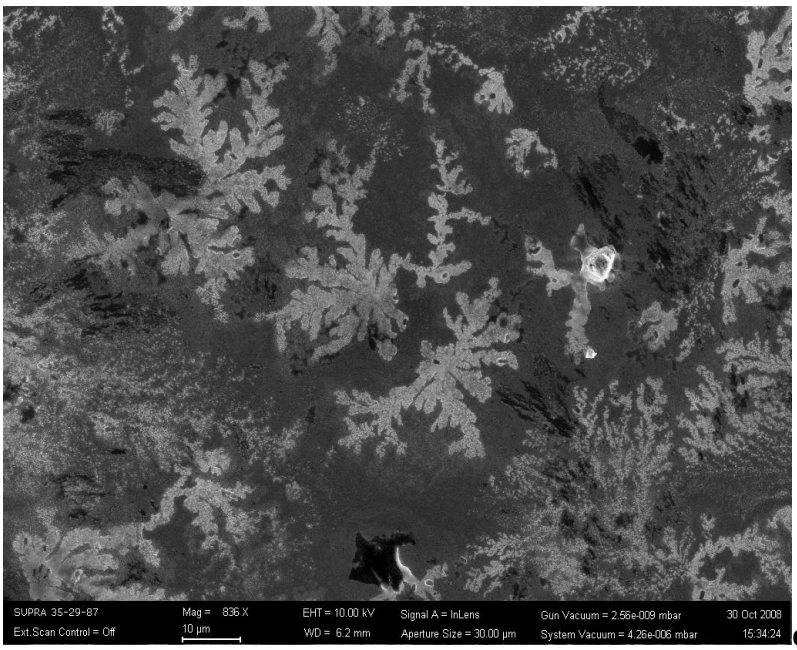

d)

(d) SEM image of bacteria immobilized on Au / mSAM2 / anti-bacterial / BSA (10 µm, Mag. 836 KX) [198]

The functionality of the biosurfaces has been demonstrated using chemically functionalized surfaces by comparison. It was developed and tested a new protocol for detecting bacteria with capacitive interdigitated immunosensor, using microfluidics platform described în Chapter 2. Also it were tested the silicon substrates compared with gold substrates. They showed a low reproducibility and a high detection limit.

After evaluation of the morphological steps of forming the bacteria onto bio surface it have been were carried out the bacteria quantization onto gold surfaces/$mSAM_2$ / anti-E. coli and the functionalized silica GOPT / anti-E. coli by means of a sandwich similar to the ELISA method.

The same method was used for functionalization of surfaces in the form of gold interdigitate lines of a chip made în the same manner as the chips hFABP tested for protein detection. It has an active gold surface structure as shown in Fig. 2.36 b.

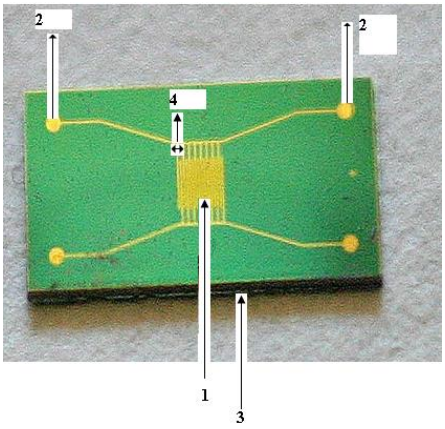

1. interdigitated gold electrodes region or active area;
2. **pads measurement (electrical contacts);**
3. the immunosensor as a total area of 7.2 mm^2;
4. each interdigitated gold electrode have a thickness of 10 µm.

Fig.2.36 b. The device used in thesis

It was followed the same principle as at immuno capacitive sensor used to detect h FABP protein so: at binding of bacteria on surfaces bio, Au / hSAM / anti-E.coli / BSA and

respectively Au / mSA1 / anti-E.coli / BSA, there is an increase in the thickness of the layers, which determines changes in total capacity on each bio surface according to the equation 2.3.

Under optimum conditions, the capacity changes were proportional to the logarithmic concentration of added bacteria onto bio surfaces, Au / mSAM2 / anti E. coli / BSA. The equation of the regression, the regression coefficient R^2 and the limit of detection for both of the electrodes are shown in Table 3.7.

Tabel.3.7. The parameters for calibration curve

Curve parameters	**Au/mSAM2/EDC/NHS/anti-*E.coli O157:H7*/BSA/bacteria *E.coli***
Equation	DC (nF) = -11,00 – 9,55 log **C** $_{E.coli}$
Regression coefficient	R^2 = 0,982
Limit of detection	120 CFU/mL

The transition from "microarray" technique "microarray" was only a matter of time, when the last 90 years, the microarray was used by Mark Schena et al. at the Stanford University for the first time in the study of DNA [3]. This method can make chips by means of which it can determine quantitatively and simultaneously, more specific biomarkers acute myocardial infarction (AMI) and among whom is the h FABP biomarker, so far very little used, which in physiologically, has the concentration of ng / ml in the blood, but his concentration it changes for a few hours after the onset of AMI, so that, depending on the value determined, the physician can precisely determine the onset and severity of the disorder.

There are very few authors who have achieved tests on the cardiac marker protein using microarray technology and, especially, there is no such microarray bio nano structured gold surface for specific detection of h FABP protein. Given these findings, developing and optimizing a strategy for detection of the h FABP protein using the microarray technique on gold surface through functionalized self-assembled layers, was another objective of this thesis.

Thus, Chapter 4 elaborates the protocol for developing a microarray chip for detection of cardiac marker protein h FABP. For demonstration of the methods of functionalization, the chip surface was carried out by printing the fluorophore-labeled h FABP antibodies (using microarray system) with the nano liter volumes and the results were calculated by fluorescence intensity of the spots. This intensity was compared to the intensity of the same labeled antibody immobilized on gold surface by physical adsorption in the same conditions.

For h FABP protein detection was used a sandwich immune reaction, so that on the surface it was filed a unlabeled antibody, the capture antibody that should recognize a specific amino acid sequence of the protein h FABP distinct compared to the antibody used for detection. Scanarea în fluorescenţă a suprafeţelor *microarray*, după această reacţie, a arătat o intensitate la fluorescenţă mult diminuată faţă de intensitatea pe care au înregistrat-o anticorpii de detecţie când s-au depus singuri pe suprafaţă. Since fluorescence intensities after immune reaction are low, we wanted to test anti-FABP complex interacting with the fluorophore and see if fluorophore conjugation procedure it did not affect the amino acid sequence of the protein responsible for binding (Fab region). The physico-chemical study (fluorescence, circular dichroism, theoretical modeling molecular) demonstrated that, indeed, conjugating the antibody IgG1 with commercial fluorophore, widely used fluorescein isothiocyanate (FITC), could affect the binding site of this protein. The experiments obtained so far have led us to the next objective

of this study, namely to develop physico-chemical complex study which compared the physico-chemical properties between a fluorescent new compound from the indandione class , 2- (2-hydroxy-5-nitrobenzylidene) -1,3 indanedionă (HNBID) and the best known, comercial used fluorophore (FITC), both in interacting with anti-hFABP, IgG_1 antibody.

The quenching constant, K_{SV}, is determined by the Stern-Volmer Equation [211]:

$$\frac{F_0}{F} = 1 + K_{SV}[Q] \quad (4.1)$$

where F_0 and F are fluorescence intensities of anti-hFABP in absence and presence of the quencher (HNBID or FITC), respectively. Stern-Volmer plots on the linear domain are displayed in Figure 4.10 (a) and the resulting K_{SV} values are given in Table 4.2. One can observe that HNBID has an approximately 2.5 higher protein quenching ability when compared to FITC. This translates into lower amounts of HNBID being needed to obtain the same effect as FITC, and thus into a smaller perturbation exerted upon the studied system.

Figure 4.10 Determination of the quenching (**a**) and binding (**b**) parameters of the HNBID–anti-hFABP (■) and FITC–anti-hFABP (□) systems.

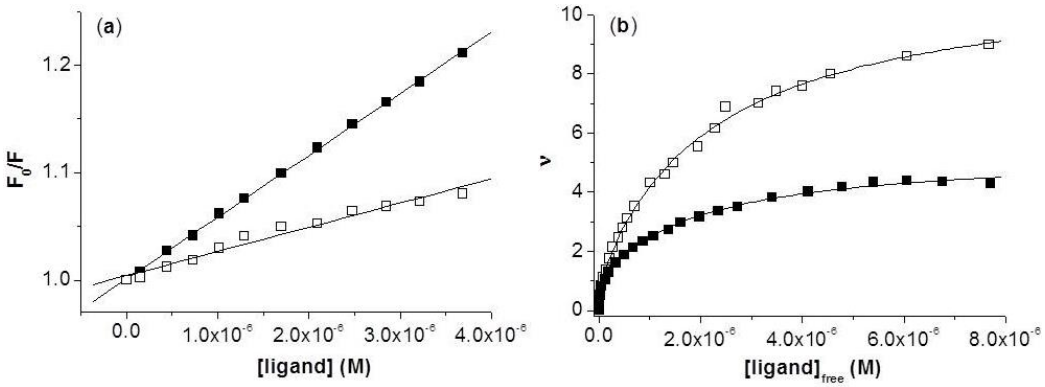

Table 4.2. Quenching and binding parameters of the HNBID–anti-hFABP and FITC–anti-hFABP systems.

Ligand	$K_{SV} \times 10^{-4}$ (M^{-1})	R [a]; SD [b]; N [c]	$K \times 10^{-6}$ (M^{-1})	n	R; SD; N
HNBID	5.75 ± 0.04	0.999; 0.002; 12	41.35 ± 16.85	1.00	0.997; 0.080; 23
			5.22 ± 0.60	4.36	
FITC	2.25 ± 0.12	0.986; 0.005; 12	50.41 ± 30.59	1.01	0.998; 0.142; 23
			0.44 ± 0.04	10.41	

Notes: [a] R = correlation coefficient; [b] SD = standard deviation of the fit; [c] N = number of experimental points.

The binding parameters are determined employing the Scatchard equation in non-linear form (4.2), considering the presence of either one (i = 1) or two (i = 2) independent sets of equivalent binding sites [212,213]:

$$\nu = \sum_i \frac{n_i K_i [ligand]_{free}}{1 + K_i [ligand]_{free}} \quad (4.2)$$

where $\nu = [ligand]_{bound}/[anti\text{-}hFABP]$ is the mean degree of binding, *i.e.*, the number of moles of ligand bound per mole of protein. The concentration of free ligand is estimated by Equation (3):

$$[ligand]_{free} = [ligand](1 - \frac{F - F_\infty}{F_0 - F_\infty}) \quad (4.3)$$

where [ligand] is the total HNBID or FITC concentration, F_0 and F are fluorescence intensities in absence and presence of the ligand, respectively, and F_∞ the fluorescence intensity of anti-hFABP at fully bound ligand. Statistically significant fits were obtained for Equation (2) when i = 2, indicating, for both ligands, the presence of two classes of binding sites: the first class consists of one binding site (n_1 = 1), *i.e.*, the high affinity site (h.a.s.), while the second class encompasses several binding sites (n_2 = 4 for HNBID and 10 for FITC) with affinities one order of magnitude lower than that of the h.a.s. (Table 4.2) **[208].** Additional confirmation of the presence of more than one class of binding site has been obtained by observing a non-linear representation (Figure S1) when plotting the Scatchard equation in linear form. By means of molecular modeling, we attempted to localize the h.a.s., as well as some of the lower affinity binding sites (Fig.4.13).

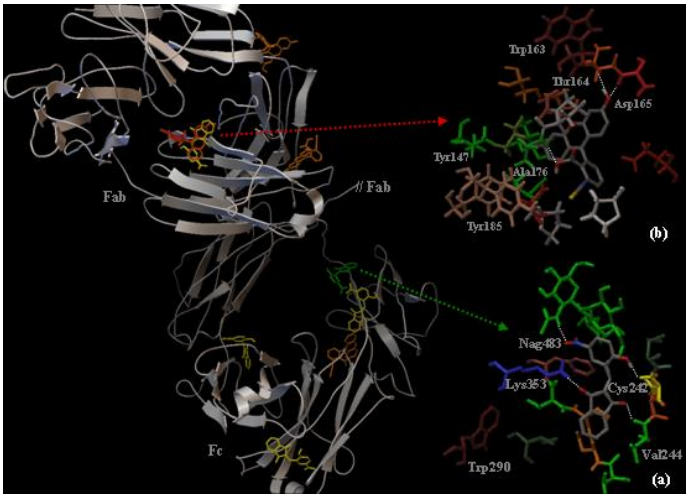

Figure 4.13. ***Left*****: The localization in the Fab and Fc regions of IgG1 of the binding sites of HNBID (high affinity binding site in Fc, in green, and low affinity binding sites in Fab and Fc, in yellow) and FITC (high affinity binding site in Fab, in red, and low affinity binding sites in Fab and Fc, in orange).** ***Right*****: IgG1 amino acid residues within a 5 Å distance from the ligand, for HNBID (a) and FITC (b); hydrogen bonds are represented by white dotted lines [208].**

This affinity of HNBID, for the antibody region containing oligosaccharide chains, could constitute an advantage as the labeling conditions might be milder.

The results recommend HNBID as a possible valuable alternative to FITC for use as fluorescent label for IgG1 anti-hFABP antibodies. Our further studies will include the labeling of anti-hFABP with HNBID, by taking advantage of the reactive groups on HNBID (-OH or -NO_2) able to bind covalently to specific functional groups on the Fc region of the antibody, and studying the antigen–antibody interaction, with the ultimate goal of developing a fluorescent sandwich microarray immunoassay for hFABP detection.

Beside low consumption of reagents and biological samples my hope is that in the near future bionanostructured surfaces will ultimately lead to the production of medical devices with high

potential for portability, important property when can track / detect biomarkers important in acute myocardial infarction or bacteria present in contaminated samples.

List of publications in the field of thesis

1. **Mihailescu, C. M.,** Stan, D., Iosub, R., Moldovan, C., & Savin, M, A Sensitive Capacitive Immunosensor for Direct Detection of Human Heart Fatt Binding Protein (H-FABP)/. *Talanta*/ *132*/ 2015/ 37-43 (impact factor 3,545/2014).

2. Stan, D., **Mihailescu, C. M.,** Savin, M., & Matei, I. (2013). Fluorescein Isothiocyanate in Interaction with Anti-hFABP Immunoglobulin G1: Fluorescence Quenching, Secondary Structure Alteration and Binding Sites Localization. *Int. J. Mol. Sci*, *14*, 3011-3025 (impact factor 2,862/ 2014).

3. Stan, D., **Mihailescu, C. M.,** Iosub, R., Moldovan, C., Savin, M., & Baciu, I. (2012). Electrochemical studies of homogeneous self-assembled monolayers versus mixed self-assembled monolayers on gold electrode for "label free" detection of heart fatty acid binding protein. *Thin Solid Films*, *526*, 143-149 (impact factor 1,759/2014).

4. Moldovan, C., **Mihailescu, C.,** Stan, D., Ruta, L., Iosub, R., Gavrila, R., & Vasilica, S. (2009). Characterization of self-assembled monolayers (SAMs) on silicon substrate comparative with polymer substrate for *Escherichia coli* O157: H7 detection. *Applied Surface Science*, *255*(22), 8953-8959 (impact factor 2,711/2014).

International journals indexed

1. **Mihailescu, C.,** Stan, D., Ruta, L., Ion, B., Moldovan, C., Schiopu, V., ... & Gavrila, R. (2008, October). Mixed-monolayers with alkane thiol on gold as substrates for microarray applications. In *Semiconductor Conference, 2008. CAS 2008. International* (Vol. 1, pp. 173-176). IEEE.

2. **Mihailescu, C.,** Baciu, I., Stan, D., Moldovan, C., Iosub, R., Dinescu, A., ... & Savin, M. (2011, October). Morphological identification through electron microscopy (SEM) and Ellipsometric studies of E. coli O157: H7 cells adsorbed onto surface. In *Semiconductor Conference (CAS), 2011 International*(Vol. 1, pp. 105-108). IEEE.

3. Stan, D., **Mihailescu, C.,** Iosub, R., Savin, M., Ion, B., & Gavrila, R. (2012, October). Development of an immunoassay for impedance-based detection of heart-type fatty acid

binding protein. In *Semiconductor Conference (CAS), 2012 International* (Vol. 1, pp. 157-160). IEEE.

Other journals in the field (whose results are not included in this thesis)

1. Simion, M.; Ruta, L.; **Mihailescu, C**.; Kleps, I.; Bragaru, A.; Miu, M.; Ignat, T.; Baciu, Ion, Porous silicon used as support for protein microarray, *Superlattices And Microstructures*, 46 (2009), 69-76 (isi 1.979).

2. D. Stan, **C. Mihăilescu,** C. Paraschivescu, **E. Oprea**, I. C. Fărcăşanu, Protein electrophoresis an important method of clinical laboratory diagnosis, Rev. Chim. 2006, 57 308-311 (isi 0.677).

3. D. Stan, I. Matei, **C. Mihailescu**, M. Savin, M. Matache, M. Hillebrand, I. Baciu "Spectroscopic Investigations of the Binding Interaction of a New Indanedione Derivative with Human and Bovine Serum Albumins"/ /Molecules/ 2009/ 14/ 1614–1626 (isi 2.416)

The results presented in other scientific events:

1. Characterized of self-assembled monolayers (SAMs) on polymer substrate comparative with silicon substrate for *E.coli detection*, Carmen Moldovan, **Carmen Mihăilescu**, Dana Stan, 15th- 19th September, 2008, EMRS Conference, Warsaw University of Technology Warsaw (Poland), Book of Abstracts, pagini 287-288.

2. Mixed Self-Assembled Monolayers (SAMs) with alkane thiol on gold as substrates for immunosensors applications /D. Stan, **C. Mihailescu**, C.Moldovan, A. Dinescu, V. Schiopu, R. Iosub, M. Savin, I. Baciu /7th International Conference on Biomedical Application of Nanotechnology, 1-4 decembrie 2010, Berlin – Germania / Book of abstracts pag. 46-48.

3. Developing of a new capacitive immunosensor for *label free* detection of *Escherichia coli* O157: H7/**C-M Mihailescu**, D. Stan, R. Iosub, , M. Savin, C. Moldovan/ Revista Romanian Laboratory Medicine /2013/21/S77-S78.

4. Porous Silicon Surfaces - a Proper Substrate for Microarray Tehnology, M. Simion, **C. Mihailescu**, L. Ruta, T. Ignat, I. Kleps, D. Stan, A. Bragaru, M. Miu, **Advances in Microarray Technology (AMT)**, poster May 2008, Spain.

SELECTIVE REFERENCES

[1]. Turner A.P.F., I. Karube, G.S. Wilson, Biosensors: Fundamentals and Applications, Oxford University Press, Oxford, **1989**, pp.24-36.

[2]. Thevenot DR, Toth K, Durst R.A, Wilson G.S., **1999**, *Pure Appl. Chem*. 7, 2333-2348.

[3]. Schena, M., Shalon, D., Davis, R. W., & Brown, P. O., *Science*, **1995**, *270*(5235), 467-470.

[101]. Zou Z., Kai J., Rust M.J., Han J., Ahn C.H., **2007**, *Sensors Actuators A*, 136, 518-526.

[101]. Boubour, E. . *Ion Transport and Electron Transfer at Self-assembled Alkylthiol/gold Monolayers*. McGill University, 2000, pp.iii.

[145]. Stan, D., Mihailescu, C. M., Iosub, R., Moldovan, C., Savin, M., & Baciu, I., 2012, *Thin Solid Films*, *526*, 143-149.

[146]. Boubour, E. (2000). *Ion Transport and Electron Transfer at Self-assembled Alkylthiol/gold Monolayers*. McGill University.

[147]. Mihailescu, C. M., Stan, D., Iosub, R., Moldovan, C., & Savin, M. (2015). *Talanta*, *132*, 37-43.

[152]. Nuzzo R.G., Korenic E.M., Dubois L.H., Allara D.L., **1990a.** *J.Phys.Chem,* 767-773.

[197]. Moldovan, C., Mihailescu, C., Stan, D., Ruta, L., Iosub, R., Gavrila, R., ... & Vasilica, S., 2009,. Applied Surface Science, 255, 8953-8959.

[198]. Mihailescu, C., Baciu, I., Stan, D., Moldovan, C., Iosub, R., Dinescu, A., ... & Savin, M. (2011, October). Morphological identification through electron microscopy (SEM) and Ellipsometric studies of E. coli O157: H7 cells adsorbed onto surface. In Semiconductor Conference (CAS), 2011 International(Vol. 1, pp. 105-108). IEEE.

[208]. **D. Stan, CM. Mihailescu, M. Savin, I. Matei, *Int. J. Mol. Sci.* 2013, *14*, 3011–3025.**

[211]. M. R. Eftink, Fluorescence quenching. Theory and applications. In *Principles of Fluorescence Spectroscopy*; Lakowicz, J.R., Ed.; Kluwer Academic/Plenum Publishers: New York, NY, USA, 1999; pp. 53–127

[212]. Scatchard, G., **1949**, *Ann. N.Y. Acad. Sci., 51,* 660–672.

[213]. Höfliger, M.M.; Beck-Sickinger, A.G. Receptor–ligand interaction. In *Protein-Ligand Interactions from Molecular Recognition to Drug Design*; Böhm, H.J., Schneider, G., Eds.; Wiley-VCH Verlag: Weinheim, Germany, 2003; p. 113.